Predict-first integrated modeling of WEST long pulse operation with combined ECRH/ECCD and LHCD

T. Fonghetti[1,2], P. Manas[1], R. Dumont[1], J-F. Artaud[1], C. Bourdelle[1], F.J. Casson[3], J. Cazabonne[1], R. Coelho[4], N. Cummings[3], L. Delpech[1], P. Maget[1], J. Morales[1], M. Schneider[5], E. Vergnaud[1] and the WEST team[6]

[1]*CEA, IRFM, F-13108 Saint-Paul-lez-Durance, France*

[2]*CNRS, Aix-Marseille Univ., PIIM UMR7345, Marseille, France*

[3]*CCFE, Culham Science Centre, Abingdon, OX14 3DB, UK*

[4]*Instituto de Plasmas e Fusao Nuclear, Instituto Superior Técnico, Universidade de Lisboa, 1049-001, Lisboa, Portugal*

[5]*ITER Organization, Route de Vinon-sur-Verdon, 13067 St. Paul-lez-Durance Cedex, France*

[6]*see http://west.cea.fr/WESTteam*

Introduction

Achieving long-pulse operation [1] is essential for developing steady-state scenarios in next-generation tokamaks such as ITER and for assessing the lifetime of highly exposed plasma-facing components. WEST, equipped with actively cooled tungsten plasma-facing components, is designed for long-duration discharges and provides up to 7 MW of Lower Hybrid Current Drive (LHCD) power [2]. In 2025, WEST achieved a record plasma duration of 1337 s and an injected energy of 2.61 GJ, supported by integrated modelling. The simulations were performed with the High-Fidelity Plasma Simulator (HFPS), an IMAS-compatible implementation of JINTRAC [3]. HFPS self-consistently predicts one-dimensional plasma profiles using JETTO, full-radius turbulent heat and particle transport from TGLF-sat2 [4], and heating and current-drive sources from the H&CD workflow [5], as fully described in [6,7]. This framework was used to optimize the operational domain in LHCD power, plasma current, and electron density, with subsequent experiments confirming the predictions [6]. Two main limitations were identified, both associated with off-axis LH deposition: hollow safety factor profiles prone to tearing modes and insufficient core electron heating, allowing radiative losses to trigger plasma collapse. The present study investigates Electron Cyclotron (EC) waves in heating and current-drive configurations, in preparation for the new 3 MW EC system [8]. Their localized and steerable heat and current sources [9] are assessed as a means of extending the WEST operational domain while optimizing the trade-off between MHD stability, stored energy, and confinement. Most of these results are detailed in [7].

Improving core power balance to avoid radiative collapses

It was shown in [10] that, in WEST, the core electron temperature can saturate below a threshold of approximately 2 keV because of strong tungsten radiative cooling. This regime, referred to as the cold branch, corresponds to a failure to overcome the tungsten radiation barrier, and eventually ends up with radiative collapses featuring a plasma disruption. It is typically observed at high density, where electron heating becomes less effective while radiative losses increase. An example is shown in Fig. 1, as the result of HFPS predictions for a plasma with a line-averaged density of 5.10^{19} m^{-3}. In the absence of EC heating (P_{EC}=0), the ratio of core radiated power (ρ<0.3) to injected RF power continues to increase during the LHCD power ramp. This behaviour results from the combination of a total radiated fraction of approximately 50%, as commonly measured by bolometry in the WEST database, and an outward displacement of the LHCD power deposition in the cold, high-density plasma. On-axis ECRH, with powers up to 0.6 MW, is therefore applied before the LHCD ramp. Remarkably, only 300 kW is sufficient to overcome the tungsten radiation barrier, restore a favourable core power balance, and access the hot branch. This result suggests that ECRH may enable high-density, long-pulse operation otherwise limited by radiative collapses. Such operation is particularly attractive in electron-heated plasmas, since electron–ion collisional energy transfer increases with density and provides the main pathway for ion heating.

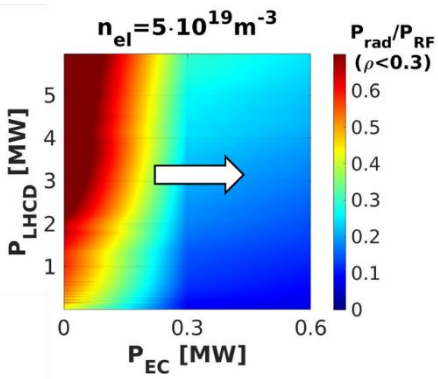

Fig 1. Heat map of the ratio of the integrated radiated power over the heat power in the core region (ρ<0.3) during LHCD power ramp-up on the y-axis and for several EC powers ranging from 0 to 0.6 MW in the x-axis.

Access to reversed-shear configurations with off-axis ECCD

The toroidal injection angle was selected to maximize the ECCD efficiency, while the poloidal angle was varied to shift the EC deposition from the magnetic axis ρ_{EC}~0 to ρ_{EC}=0.5. Different EC power levels were applied to an LHCD-only reference discharge with I_P=300 kA, P_{LHCD} = 2 MW, and n_{el}=3.10^{19} m^{-3} to identify the best trade-off between MHD stability and plasma performance. The following analysis focuses on cases with a total injected power of 3.5 MW. As shown in Fig. 2(a), ECCD modifies the LHCD deposition profile, consistently with previous observations reported in [11]. Identifying the mechanisms responsible for this interaction would nevertheless require first-principles modelling of the electron distribution function. The resulting redistribution of the driven current modifies the current-density, safety-factor, and magnetic-shear profiles within (ρ<0.5), as shown in Fig. 2(b). Depending on the EC deposition location, reversed-shear configurations can be obtained with the q-profile reversal located closer to or farther from the magnetic axis. Although the reduced turbulent transport allows locally steeper temperature gradients than in the monotonic-q configuration, the limited heating power deposited inside the low-transport region, as outlined in Fig. 2(c) by the filled area, strongly restricts the resulting increase in stored energy. Consequently, the on-axis ECCD case (ρ_{EC}~0) exhibits a larger stored energy because of its stronger central electron heating and larger core temperature gradients. To exploit the improved confinement associated with reversed shear, an additional on-axis ECRH source is therefore introduced. When the q-profile is held fixed, the reversed-shear configuration outperforms the on-axis ECCD case with same levels of injected power, as substantially larger core temperature gradients can be sustained. However, when the current-density and q-profiles are evolved self-consistently, the enhanced temperature gradients increase the bootstrap current, weaken the q-profile reversal, and thereby mitigate the reduction in turbulent transport. Exploiting reversed shear therefore requires careful optimization of the LHCD and ECCD deposition profiles, and access to such an improved-confinement configuration is likely to remain challenging.

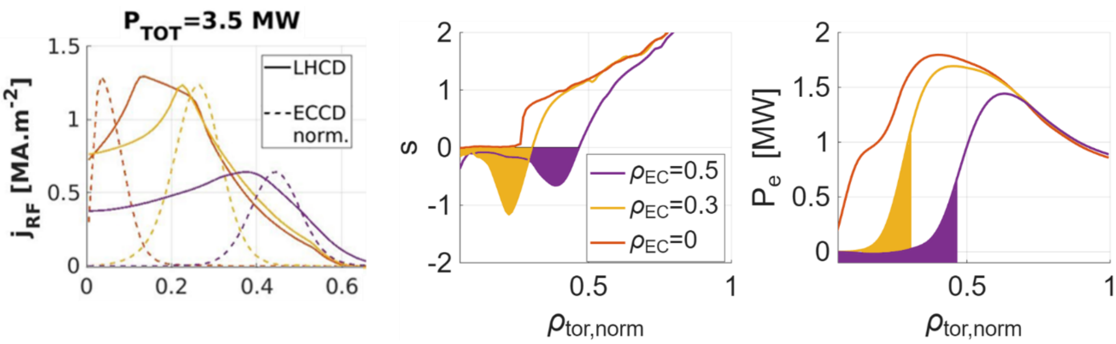

Fig 2. (a) LHCD current density (plane) and normalized ECCD to the maximum LHCD current (dashed), (b) magnetic shear and (c) electron heat power profiles for the three different ECCD configurations at P_{TOT}=3.5 MW; ρ_{EC}~0 (red), ρ_{EC}=0.3 (yellow) and ρ_{EC}=0.5 (purple). In (b) and (c) the reversed-shear region is filled.

A stable plasma scenario studied with linear resistive MHD analysis

Experimental observations in Tore Supra and WEST have shown that reversed q-profiles are particularly prone to MHD instabilities, most notably (3,2) and (2,1) double tearing modes [12]. In such unstable plasmas, both confinement and current-drive efficiency are degraded [13], potentially leading to a disruption. To assess the stability of the configurations presented in Fig. 2, additional HFPS simulations are performed in which the EC source is switched off. The plasmas consequently relax towards the 2 MW LHCD-only configuration through resistive diffusion of the current-density profile. During this relaxation, a range of intermediate plasma configurations are obtained, and their linear resistive MHD stability is evaluated using the MARS code [14]. The calculated growth rates of the (3,2) and (2,1) tearing modes indicate that the most unstable configurations occur when the q-profile reversal is located close to the corresponding rational surface, or equivalently when q_{min} lies slightly below this surface while

q_0 remains high. In contrast, both the monotonic q-profile obtained with on-axis ECCD and the reversed-shear configuration with q_{min} greater than 2, obtained with off-axis ECCD, are found to be linearly stable. However, the trajectory followed to reach these stable configurations is also important. Maintaining q_{min} above 2 throughout the discharge is challenging and requires precise optimization of the current and heating power ramp-up. By contrast, progressively decreasing q_0 towards 1 from an initially reversed-shear configuration remains stabilizing along the entire trajectory and appears more accessible from an operational perspective.

The addition of on-axis ECCD as an alternative to LHCD-only configuration

Overall, given the risk of triggering MHD instabilities and the need for precise optimization of the power ramp-up and launcher settings in off-axis ECCD configurations, on-axis ECCD appears to be the most viable alternative to LHCD-only operation. Fig. 3 compares both configurations at similar total injected power. Only 200 kW of additional power is required in the on-axis ECCD case to achieve fully non-inductive operation, while the stored energy is increased by approximately 10% without further degradation of confinement with increasing power. The configuration is also more stable against double tearing modes, owing to a monotonic q-profile approaching q = 1 in the core. Finally, the additional central electron heating provided by on-axis ECCD improves the core power balance and could facilitate access to high-density operation.

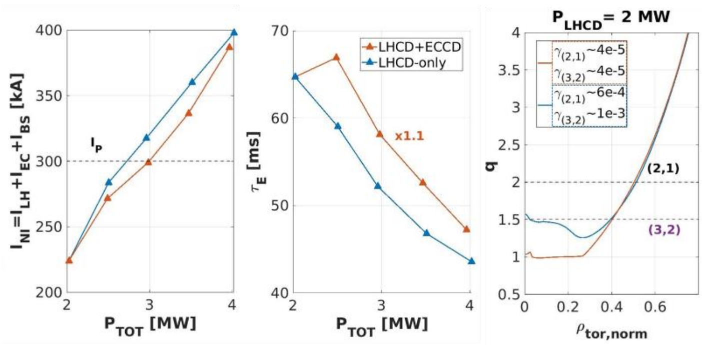

Fig 3. (a) Non-inductive current-drive and (b) energy confinement time against the total power for the combined on-axis ECCD and LHCD (red) and the LHCD-only (blue) configurations. In (a) the dashed line represents the total plasma current. (c) q-profile for the LHCD-only configuration at 2 MW (blue) compared to the one with additional 1.5 MW of on-axis ECCD (red). The associated growth rates for (2,1) and (3,2) tearing modes are provided in the legend.

References

[1] X. Litaudon, et al., Nucl. Fusion, 64, 015001 (2024).
[2] J. Bucalossi, et al. Nucl. Fusion, 62, 042007 (2022).
[3] M. Romanelli, et al., Plasma and Fusion Research, 9, 3403023 (2014).
[4] C. Angioni, et al., Nucl. Fusion, 63, 126035 (2022).
[5] M. Schneider, et al., Nucl. Fusion, 61, 126058 (2021).
[6] T. Fonghetti, et al., Nucl. Fusion, 65, 056018 (2025).
[7] T. Fonghetti, et al., Nucl. Fusion, 66, 066006 (2026).
[8] L. Delpech, et al, Fusion Engineering and Design, 186, 113360 (2023).
[9] T. Fonghetti, et al., EPJ Web of Conferences, 277, 02006 (2023).
[10] J. Morales, et al, Nucl. Fusion, 65, 106003 (2025)
[11] W. Choi, et al., Annual Meeting of the APS Division of Plsma Phys., Oral contribution (2024).
[12] P. Maget, Nucl. Fusion, 45, 69-80 (2005).
[13] Y. Peysson and Tore Supra Team, Nucl. Fusion, 41, 1703 (2001).
[14] P. Maget, et al., Plasma Phys. Control. Fusion, 67, 045005 (2025).